20-nm-resolution soft x-ray microscopy demonstrated by use of multilayer test structures

Weilun Chao

Center for X-ray Optics, Lawrence Berkeley National Laboratory, Berkeley, California 94720-8199, and Department of Electrical Engineering and Computer Sciences, 211 Cory, University of California, Berkeley, Berkeley, California 94720-1770

Erik Anderson, Gregory P. Denbeaux, Bruce Harteneck, J. Alexander Liddle, Deirdre L. Olynick, Angelic L. Pearson, and Farhad Salmassi

Center for X-ray Optics, Lawrence Berkeley National Laboratory, Berkeley, California 94720-8199

Cheng Yu Song

National Center for Electron Microscopy, Lawrence Berkeley National Laboratory, Berkeley, California 94720-8250

David T. Attwood

Center for X-ray Optics, Lawrence Berkeley National Laboratory, Berkeley, California 94720-8199, and Department of Electrical Engineering and Computer Sciences, 211 Cory, University of California, Berkeley, Berkeley, California 94720-1770

Received April 22, 2003

A spatial resolution of 20 nm is demonstrated at 2.07-nm wavelength by use of a soft x-ray microscope based on Fresnel zone plate lenses and partially coherent illumination. Nanostructural test patterns, formed by sputtered multilayer coatings and transmission electron microscopy thinning techniques, provide clear experimental results.

OCIS codes: 180.7460, 340.7460, 110.4980.

Soft x-ray microscopy, based on Fresnel zone plates,[1] is under active pursuit worldwide.[2] The short wavelength provides a path to improved spatial resolution, whereas the high photon energy allows elemental and chemical identifications based on sharp atomic resonances.[1] In this Letter we report a significant step forward in high spatial resolution imaging, based on improved zone plates, partially coherent illumination, and the use of a soft-x-ray-sensitive CCD detector.

The soft x-ray microscope, XM-1,[3,4] uses bend magnet radiation from the Advanced Light Source[5] for imaging. By use of illumination between 300 and 1800 eV ($\lambda = 4-0.7$ nm), the microscope is capable of imaging nanomagnetic structures at absorption edges of various constituents,[6] electromigration in interconnects,[7] wet environmental samples,[8,9] and thick, unstained, and labeled biological specimens in aqueous environments.[10] Tomographic imaging has also been performed to obtain three-dimensional information.[7,11]

The microscope is shown schematically in Fig. 1. It is a full-field transmission microscope consisting of a condenser and an imaging lens. The imaging lens of the microscope, the microzone plate (MZP), projects a full-field image onto a 1024 × 1024 pixel soft-x-ray-sensitive CCD detector. An upstream condenser zone plate (CZP) provides partially coherent illumination of the samples. The degree of partial coherence, σ, of the illumination is discussed later in this Letter. Because of the strong chromatic aberration and multiple diffraction orders of zone plates, the central region of the condenser is blocked by a stop, and a small pinhole is used near the sample plane. This yields monochromization ($\lambda/\Delta\lambda$) between 500 and 700, over a 10-μm-diameter field of view.[4] The parameters of the condenser and MZPs are as follows: MZP: Δr_{MZP} (outermost zone width) = 25 nm, 300 zones, 30-μm diameter; CZP: $\Delta r_{\mathrm{CZP}} = 60$ nm, 41,700 zones, 10-mm diameter, 5-mm-diameter central stop.

In a perfect full-field microscope, spatial resolution is determined by the wavelength, the numerical aperture of the imaging lens (NA_i), and, to a lesser degree, by partially coherent illumination. For a zone plate, NA_i is set by the outermost zone width and the wavelength,[1] $\mathrm{NA}_i = \lambda/(2\Delta r_{\mathrm{MZP}})$. A key to achieving

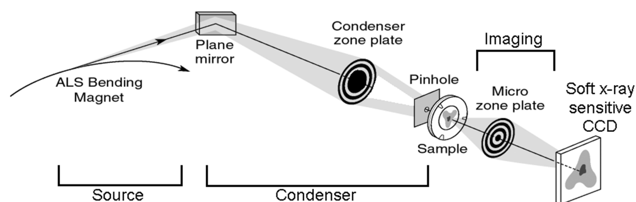

Fig. 1. Schematic diagram of the soft x-ray, full-field imaging microscope, XM-1, at the Advanced Light Source (ALS).

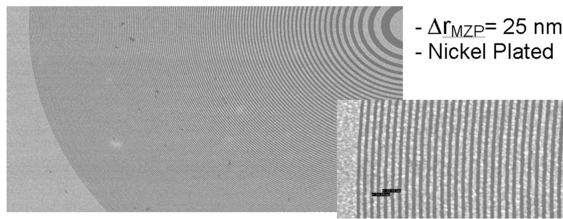

Fig. 2. Scanning electron microscope micrograph of a 25-nm outermost-zone-width MZP.

high spatial resolution is the fabrication of zone plates with fine zone widths, good circularity, high zone placement accuracy,[12] and sufficient thickness for reasonable diffraction efficiency. Both the MZP (Fig. 2) and the CZP in XM-1 are fabricated in-house with electron-beam lithography.[13] The electron-beam lithography tool, the Nanowriter, has excellent zone placement accuracy (<6 nm) and circularity by use of a pattern generator specially designed for patterning curved structures. A bilayer resist process[14] has been utilized, permitting fabrication of relatively thick zone plates, 80 nm of nickel in this case.

The image intensity acquired at XM-1 is a nonlinear convolution[15–17] of the object's transmission function, the MZP's pupil function, and, more importantly, the spatial coherence in the object plane, which can substantially alter the image quality for a given MZP. For an incoherent bend magnet radiation source, the mutual intensity in the object plane and the amplitude impulse response of the MZP are related to each other by the degree of partial coherence[16] σ. The value of this parameter is determined by the ratio of the numerical aperture of the condenser lens (NA_c) to that of the objective lens (NA_i):

$$\sigma = \frac{\mathrm{NA}_c}{\mathrm{NA}_i} = \frac{\Delta r_{\mathrm{MZP}}}{\Delta r_{\mathrm{CZP}}}\,. \tag{1}$$

For coherent imaging in which a plane wave illuminates the sample, NA_c and σ are zero. For incoherent imaging, in which the angular illumination of the sample is large relative to the acceptance angle of the MZP, σ approaches unity or larger. For the resolution measurement described here, a partially coherent illumination is used, with σ equal to $25/60\ \mathrm{nm} = 0.42$.

Here we define spatial resolution to be the half-period of a periodic line and space pattern that exhibits a 26.5% modulation in its image.[16] This 26.5% modulation equals that of the Rayleigh criterion for imaging two mutually incoherent point sources with a circular objective. Resolution is often expressed as $k_1\lambda/(\mathrm{NA}_i)$, which for a zone plate is equal to $2k_1\Delta r_{\mathrm{MZP}}$. The value of k_1 is determined by σ and aberrations. Theoretically, the diffraction-limited value of k_1 for opaque periodic equal lines and spaces decreases from 0.5 in a coherent system to 0.28 in an "incoherent" system with σ equal to unity. Thus with partially coherent imaging, the spatial resolution can be better (smaller) than the outermost zone width of the MZP.

Periodic line and space patterns and elbow patterns that allow simultaneous observation of resolution in two orthogonal directions have been fabricated in the past with the Nanowriter. As a result, it was impossible to obtain test patterns with features smaller than the finest zone of the MZP to test the microscope's resolution completely. Our new test patterns are multilayer coatings,[1,18] fabricated with magnetron sputtering.[19] Processed by thinning techniques, these patterns allow us to achieve straight-line patterns with periods down to 10 nm and with an arbitrary aspect ratio. A variety of multilayer material pairs are available to meet the specific needs of resolution tests, such as material contrast at a given wavelength. For the results reported here, we used multilayer coatings composed of forty chromium/silicon bilayer pairs, with periods of 40 and 50 nm. By use of Cu K_α x-ray reflectometry ($\lambda = 0.154$ nm), the coatings' periods were measured to be 39.0 and 48.6 nm, respectively. The samples were processed with conventional transmission electron microscopy preparation techniques[20] to have sufficient transparency for x-ray imaging. The multilayer coatings were sandwiched between two silicon blocks, thinned, and spherically polished by use of both mechanical and ion-milling techniques to form a 200-μm-thick disk, exposing a multilayer cross section. This disk has concave impressions on both sides, and the multilayer cross section, the test pattern, has a thickness that radially increases from zero at the center (a hole) to full thickness. For optimal contrast, a thickness of 200 nm was selected, yielding 80% transmission in silicon and 5% in chromium at 600 eV ($\lambda = 2.07$ nm), just above the Cr L_2 absorption edge. Phase effects are negligible in this case.

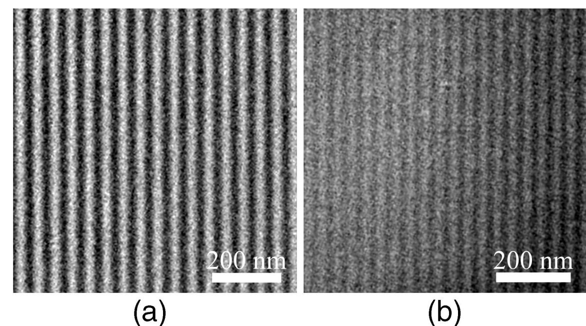

Fig. 3. Soft x-ray image of the (a) 24.3-nm half-period and (b) the 19.5-nm half-period multilayer test pattern taken at 600 eV ($\lambda = 2.07$ nm).

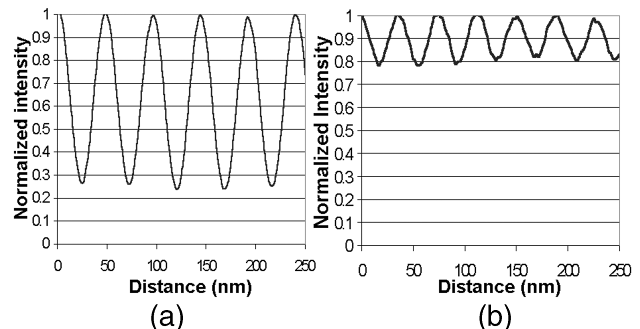

Fig. 4. (a) Lineout of the 24.3-nm half-period image shows a normalized modulation, averaged along the pattern, of 73–76%. (b) Lineout of the 19.5-nm half-period image shows a normalized modulation of 20%.

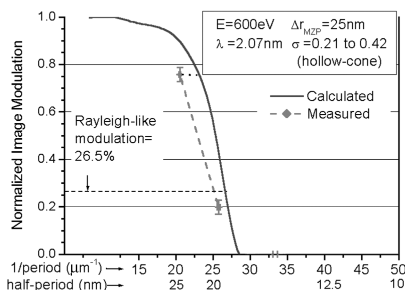

Fig. 5. Simulated modulation transfer function for XM-1 with hollow-cone, partially coherent illumination. The measured modulations from Fig. 4 are also shown. The horizontal errors for 19.5- and 24.3-nm half-periods are ± 0.2 and $\pm 0.3\ \mu\text{m}^{-1}$. The calculated resolution is 19 nm. A straight line through the two data points indicates that XM-1 has a resolution of 20 nm or 1.1 times the diffraction-limited performance.

Figures 3(a) and 3(b) show soft x-ray images of the 24.3- and 19.5-nm half-period multilayer test patterns obtained at 600 eV. Their background-corrected lineouts, averaged along the patterns, are shown in Fig. 4. The normalized measured x-ray modulations are 75% and 20% for these two half-periods.

Figure 5 shows a calculated modulation transfer function for this microscope and the two measured data points. We performed the calculation for periodic Cr/Si of equal widths using the SPLAT computer program,[21] which evaluates the Hopkins theory of partially coherent imaging[15–17] by use of numerical integration (adaptive quadrature). For these calculations, monochromatic, hollow-cone[22] radiation that uniformly illuminates the object is assumed. The calculated modulations at 24.3- and 19.5-nm half-periods are 89% and 43%, respectively. Connecting the two measured points by a straight line, a Rayleigh-like modulation of 26.5% occurs at a half-period of 20 nm, whereas the calculated modulation transfer function achieves this modulation at 19 nm. Based on these comparisons, we conclude that the spatial resolution of XM-1 is 20 nm, or 1.1 times the diffraction-limited performance.

In conclusion, the achievement of 20-nm resolution soft x-ray microscopy, based on high-quality Fresnel zone plates and partially coherent illumination, was demonstrated by use of new multilayer test patterns. A wide range of applications are currently being pursued with the microscope.

The authors thank Velimir Radmilovic and Eric Stach, National Center for Electron Microscopy, Lawrence Berkeley National Laboratory, for assistance with the test sample preparation, the Department of Energy's Office of Basic Energy Sciences, and the Defense Advanced Research Projects Agency for their generous support. W. Chao's e-mail address is wlchao@lbl.gov.

References

1. D. Attwood, *Soft X-Rays and Extreme Ultraviolet Radiation* (Cambridge University, Cambridge, England, 1999).
2. J. Susini, D. Joyeux, and F. Polack, eds., J. de Physique IV (EDP Sciences, Les Ulis, France, 2003).
3. W. Meyer-Ilse, H. Medecki, L. Jochum, E. Anderson, D. Attwood, R. Balhorn, M. Moronne, D. Rudolph, and G. Schmahl, Synchrotron Radiat. News **8,** 22 (1995).
4. G. Denbeaux, E. Anderson, W. Chao, T. Eimüller, L. Johnson, M. Köhler, C. Larabell, M. Legros, P. Fischer, A. Pearson, G. Schütz, D. Yager, and D. Attwood, Nucl. Instrum. Methods Phys. Res. A **467–468,** 841 (2001).
5. N. Smith, Phys. Today **54**(1), 29 (2001), www.als.lbl.gov.
6. P. Fischer, T. Eimuller, G. Schutz, M. Kohler, G. Bayreuther, G. Denbeaux, and D. Attwood, J. Appl. Phys. **89,** 7159 (2001).
7. G. Schneider, M. A. Meyer, G. Denbeaux, E. Anderson, B. Bates, A. Pearson, C. Knöchel, D. Hambach, E. A. Stach, and E. Zschech, J. Vac. Sci. Technol. B **20,** 3089 (2002).
8. S. C. B. Myneni, J. T. Brown, G. A. Martinez, and W. Meyer-Ilse, Science **286,** 1335 (1999).
9. K. E. Kurtis, W. Meyer-Ilse, and P. J. M. Monteiro, Corros. Sci. **42,** 1327 (2000).
10. W. Meyer-Ilse, D. Hamamoto, A. Nair, S. A. Lelievre, G. Denbeaux, L. Johnson, A. L. Pearson, D. Yager, M. A. Le Gros, and C. A. Larabell, J. Microsc. **201,** 395 (2001).
11. C. A. Larabell and M. A. Le Gros, Lawrence Berkeley Laboratory, University of California at Berkeley, Berkeley, Calif. (personal communication, 2002).
12. For minimal aberration, the zone placement error should be limited to one third of the smallest zone width.
13. E. H. Anderson, D. L. Olynick, B. Harteneck, E. Veklerov, G. Denbeaux, W. Chao, A. Lucero, L. Johnson, and D. Attwood, J. Vac. Sci. Technol. B **18,** 2970 (2000).
14. D. L. Olynick, E. H. Anderson, B. Harteneck, and E. Veklerov, J. Vac. Sci. Technol. B **19,** 2896 (2001).
15. H. H. Hopkins, Proc. R. Soc. London Ser. A **217,** 408 (1953).
16. M. Born and E. Wolf, *Principles of Optics* (Cambridge University, New York, 1999), pp. 441, 596–606.
17. J. Goodman, *Statistical Optics* (Wiley, New York, 2000), pp. 303–324.
18. T. W. Barbee, S. Mrowka, and M. C. Hettrick, Appl. Opt. **24,** 883 (1985). For other multilayer material combinations see www.cxro.lbl.gov/multilayer/survey.html.
19. J. H. Underwood, E. M. Gullikson, and K. Nguyen, Appl. Opt. **32,** 6985 (1993).
20. J. C. Bravman and R. Sinclair, J. Electron Microsc. Tech. **1,** 53 (1984).
21. K. K. H. Toh and A. R. Neureuther, Proc. SPIE **772,** 202 (1987).
22. The central stop of a CZP creates a hollow-cone illumination with σ values from 0.21 to 0.42.